WWW.IJRPR.COM

International Journal of Research Publication and Reviews

Journal homepage: www.ijrpr.com ISSN 2582-7421

CFD Analysis of Reusable Launch Vehicle during Re-Entry

***V.Keerthivasan*[a] , *S.Nagarajan*[b]**

[a]Assistant professor,Department of Aeronautical Engineering,Parisutham Institute of Technology and Science,Thanjavur-613006,Tamilnadu-India.
[b]Assistant professor,Department of Aeronautical Engineering,Parisutham Institute of Technology and Science,Thanjavur-613006,Tamilnadu-India.

A B S T R A C T

This paper deals with the design of Reusable launch vehicle (RLV) to investigate the re-entry characteristics like reentry temperature fluctuations, pressure variations and mach number at Supersonic velocities. Hence an accurate computational analysis of these flows requires to find out the best materials for the construction of RLV by using CFD software's such as ICEM CFD, CFX-PRE, CFX-SOLVER, CFX-POST. In this present work, Reusable launch vehicle (space shuttle) is designed by ICEM CFD and analysis be done through CFD with three different high Mach numbers to analyse the flow pattern, temperature fluctuations and other re-entry characteristics of RLV or space shuttle at supersonic velocities. In addition to this, Ultra high temperature materials like Silicon dibromide ($SiBr_2$) and zirconium diboride (ZrB_2), has high ablative properties are commonly used as heat shield in intercontinental ballistic missile, as thermal shielding of RLV/space shuttle, instead of conventionally used silicon based thermal protection systems.

Keywords: Reusable launch vehicle (RLV), Auxiliary Power Unit (APU), Silicon dibromide ($SiBr_2$) and zirconium diboride (ZrB_2).

1. Introduction

A reusable launch system (also known as a reusable launch vehicle, or RLV) is a launch system that can send a launch vehicle into space many times. Orbital RLVs are anticipated to offer a low-cost and extremely reliable means of accessing space. Reusability, on the other hand, entails weight penalties such as non-ablative re-entry shielding and maybe a stronger construction to withstand repeated uses, and given the lack of experience with these vehicles, the real costs and reliability have yet to be determined.

Fig.1 - Space Shuttle

* *V.Keerthivasan*. Tel.: +91-6381094524
E-mail address: keerthi.pits@gmail.com

The Space Shuttle was a partially reusable low-Earth-orbital spacecraft system that was operated by NASA as part of the Space Shuttle program. The Space Transportation System (STS) was the official program name, derived from a 1969 concept for a reusable spaceship system, of which it was the only item funded for development. In 1981, the first of four orbital test flights took place, followed by operational flights in 1982. From 1981 to 2011, they were utilized on a total of 135 flights launched from Florida's Kennedy Space Center (KSC).

2. Material Selection

On the Orbiter, a variety of Thermal Protection System materials were utilised. Tiles, advanced flexible reusable surface insulation, reinforced carbon-carbon, and flexible reusable surface insulation were among the materials used. High-emissivity coatings were utilized on all of these materials to achieve optimum rejection of incoming convective heat via radioactive heat transfer. The vehicle's temperature was used to make the decision. In locations where the temperature dropped below 1,260°C (2,300°F).

2.1. Tiles

The tiles for the shuttle were inspired by work done at Lockheed Missiles & Space Company in the early 1960s. The goal of this project is to build an active wedge nozzle to reduce jet noise. A black borosilicate glass coating with an emission value greater than 0.8 was utilized on high-temperature reusable surface insulation tiles that covered portions of the vehicle where temperatures reached up to 1,260°C (2,300°F).

2.2 . Reinforced Carbon-Carbon

The temperature extremes on the nose cap and wing leading edge of the Orbiter required a more sophisticated material that would operate over a large spectrum of environments during launch, ascent, on-orbit operations, re-entry and landing. Since carbon oxidizes at elevated temperatures, a silicon di boride coating is used to protect the carbon substrate. Any oxidation of the substrate directly affects the strength of the material and, therefore—in the case of the Orbiter— had to be limited as much as possible to ensure high performance over multiple missions. Silicon di boride is formed by converting the outer two plies of the carbon-carbon material through a diffusion coating process, resulting in a stronger coating-to-substrate interlinear strength. As a result of the silicon di boride formation, which occurs at temperatures of 1,648°C (3,000°F), craze cracks develop in the coating on cool-down as the carbon substrate and coating have a different coefficient of thermal expansion.

2.3. Re-Entry Heat Shields

Re-entry heat shields on these vehicles are often proposed to be some sort of ceramic and/or carbon-carbon heat shields, or occasionally metallic heat shields (possibly using water cooling or some sort of relatively exotic rare earth metal.)Some shields would be single use ablatives and would be discarded after re-entry's newer Thermal Protection System (TPS) technology was first developed for use in steering fins on ICBM MIRVs. Given the need for such warheads to re-enter the atmosphere swiftly and retain hypersonic velocities to sea level, researchers developed what are known as SHARP materials, typically hafnium di boride and zirconium di boride, whose thermal tolerance exceeds 3600 C. SHARP equipped vehicles can fly at Mach 11 at 30 km altitude and Mach 7 at sea level. The sharp-edged geometries permitted with these materials also eliminate plasma shock wave interference in radio communications during re- entry. SHARP materials are very robust and would not require constant maintenance, as is the case with technologies like silica tiles, used on the Space Shuttle, which account for over half of that vehicles maintenance costs and turnaround time.

3. Computational Work

3.1. 3D modelling

3d model of Reusable Launch Vehicle system has been designed with ANSYS ICEM CFD. ANSYS CFX is more than just a powerful CFD code. Integration into the ANSYS Workbench platform provides superior bi-directional connections to all major CAD systems, powerful geometry modification and creations tools with ANSYS Design Modeller, advanced meshing technologies in ANSYS Meshing, and easy drag-and-drop transfer of data and results to share between applications. The first thing to do when creating a structured grid is to create the geometry or a.tin file in ICEM.

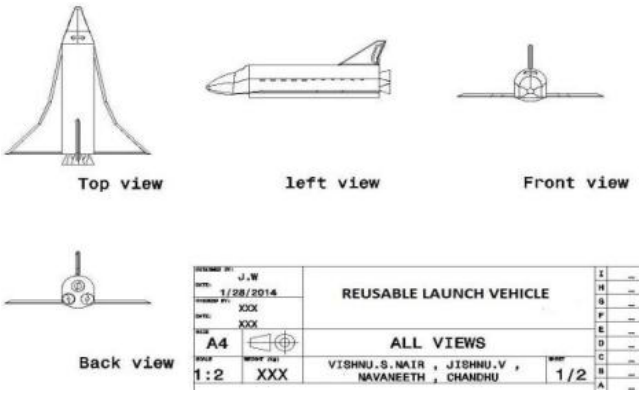

Fig.2 - Design Configuration of RLV

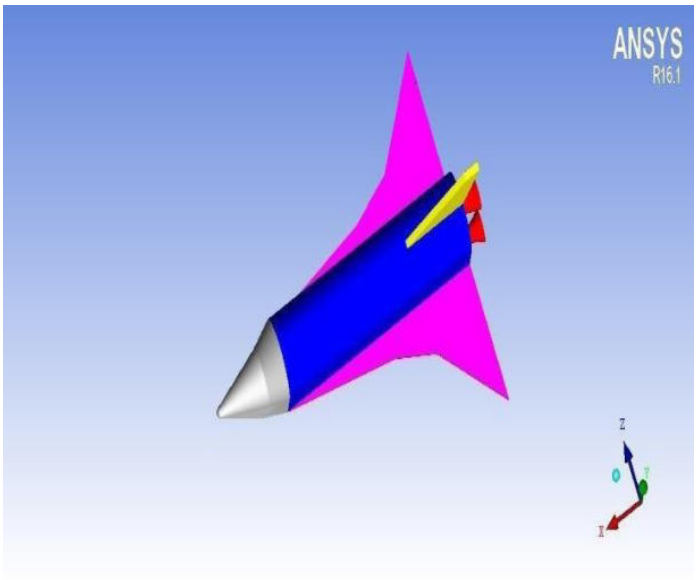

Fig.3 - RLV Model from ICEM CFD

3.2.CFD Analysis

Computational Fluid Dynamics (CFD) is an integral part of aerodynamic design process along with wind tunnel testing and engineering methods. From the design parameters and by using ICEM CFD software RLV model is imported to the ANSYS CFX software.
Control volume is created using appropriate points, curves and surfaces.

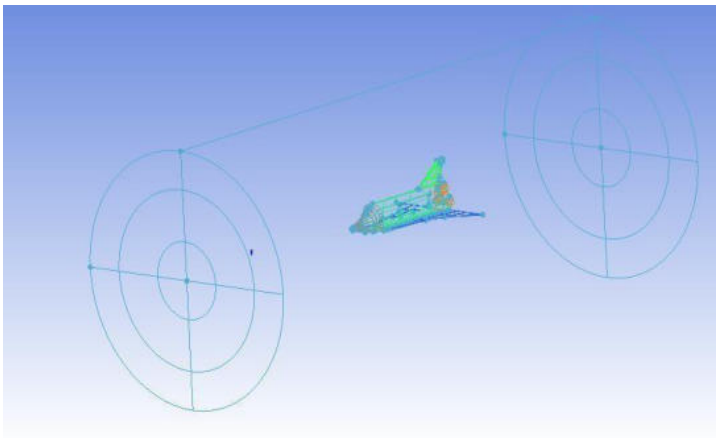

Fig.4 - Creation of control volume.

Parts are to be created to naming such as nose, wings, fuselage, vertical tail, inlet, outlet, walls. Bodies are to be created to specify the fluid/solid which is used.

To create mesh on the geometry follows the procedure as below

Mesh>global mesh setup>set the size of the meshing element>apply>dismiss Part mesh setup>set mesh size to get fine mesh>apply>dismiss

Compute mesh>mesh type-tetra/mixed>mesh method robust>compute>dismiss

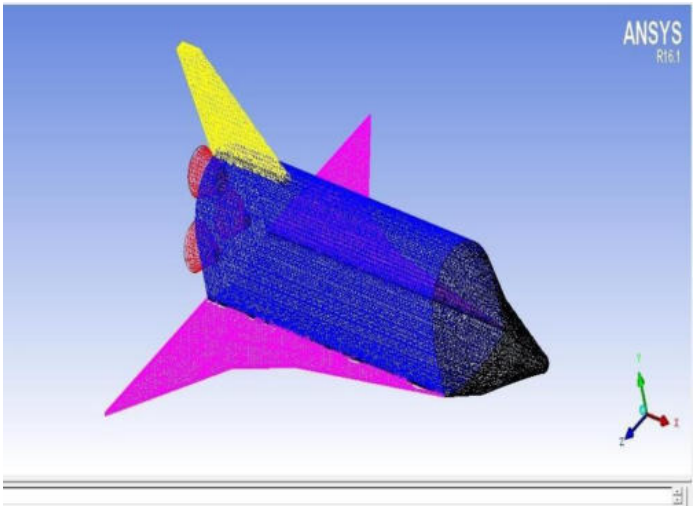

Fig.5 - Meshing of RLV.

ANSYS CFX contains three division such as pre-processor, post processor, and solver. In CFX-pre we need to set the boundary conditions for inlet, outlet, and symmetry.
After creating the domains and boundaries, and giving the necessary boundary conditions.

Table 3.2.1 Mesh Report

Domain	Nodes	Elements
Air	305227	1526487
Solid	7544	32625
All Domains	312771	1559112

4. Analysis Results

4.1. Mach Number Contour for $SiBr_2$ at Mach 1.5

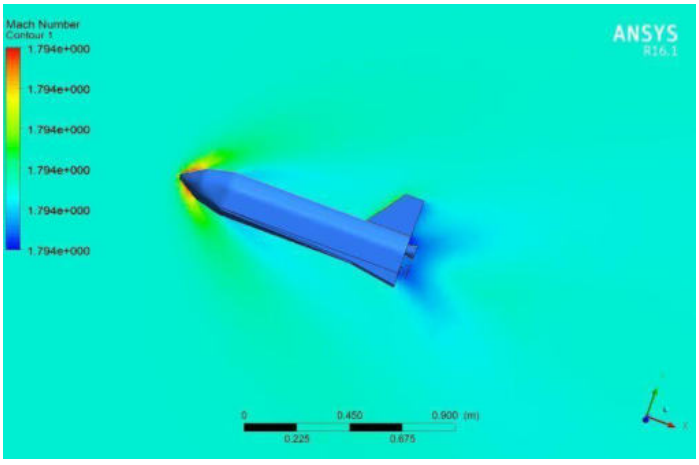

Fig.6 - Mach Number Contour for $SiBr_2$ at Mach 1.5

4.2. Temperature Contour for $SiBr_2$ at Mach 1.5

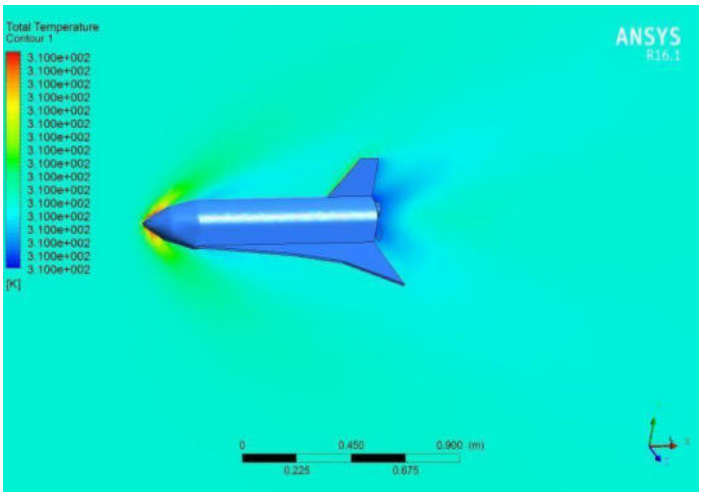

Fig.7 - Temperature Contour for $SiBr_2$ at Mach 1.5

4.3. Total Pressure Contour for $SiBr_2$ at Mach 1.5

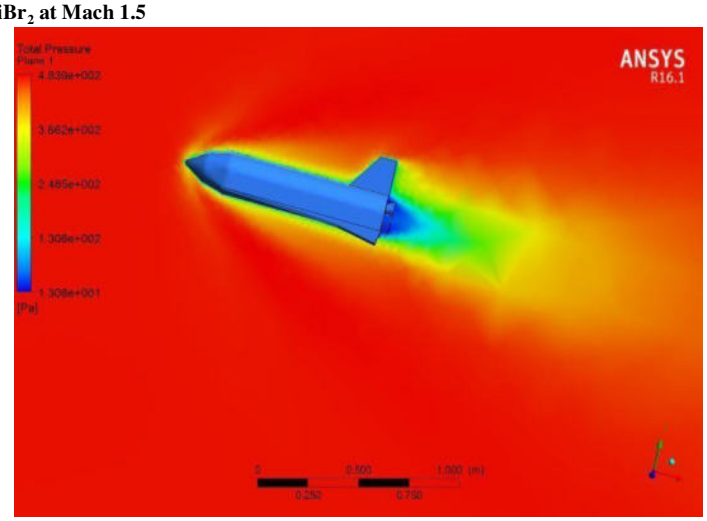

Fig.8 - Total Pressure Contour for $SiBr_2$ at Mach 1.5

4.4. Mach Number Contour for $SiBr_2$ at Mach 3

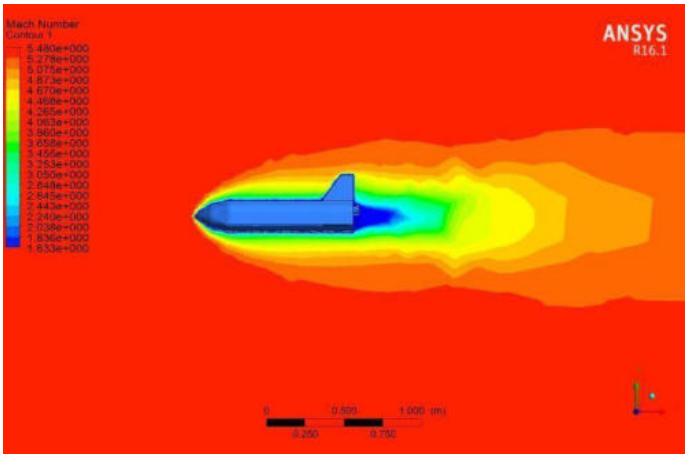

Fig.9 - Mach Number Contour for $SiBr_2$ at Mach 3

4.5. Temperature Contour for $SiBr_2$ at Mach 3

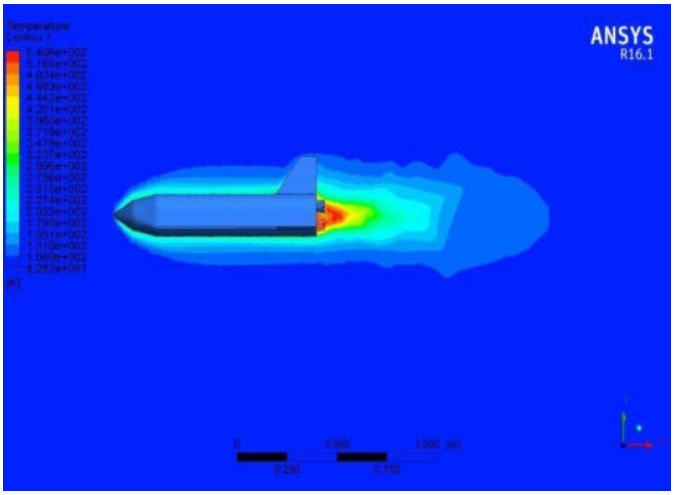

Fig.10 - Temperature Contour for $SiBr_2$ at Mach 3

4.6. Total Pressure Contour for $SiBr_2$ at Mach 3

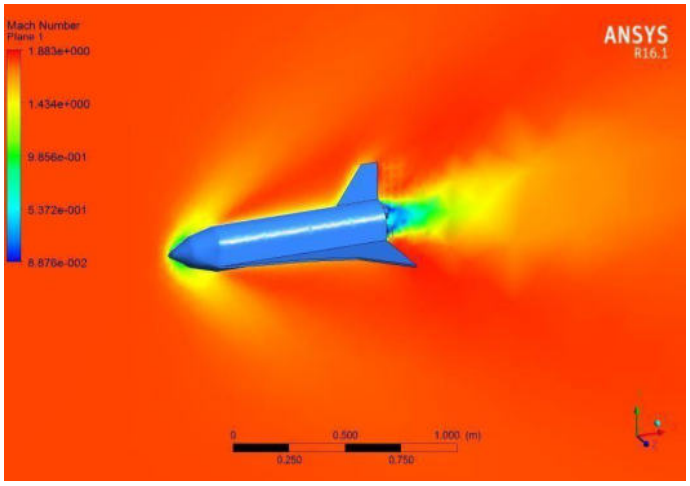

Fig.11 - Total Pressure Contour for $SiBr_2$ at Mach 3

4.7. Mach Number Contour for ZrB_2 at Mach 1.5

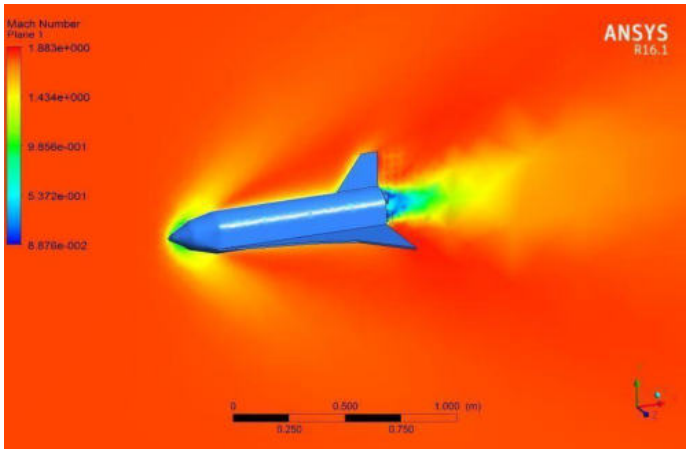

Fig.12 - Mach Number Contour for ZrB_2 at Mach 1.5

4.8. Total Pressure Contour for ZrB_2 at Mach 1.5

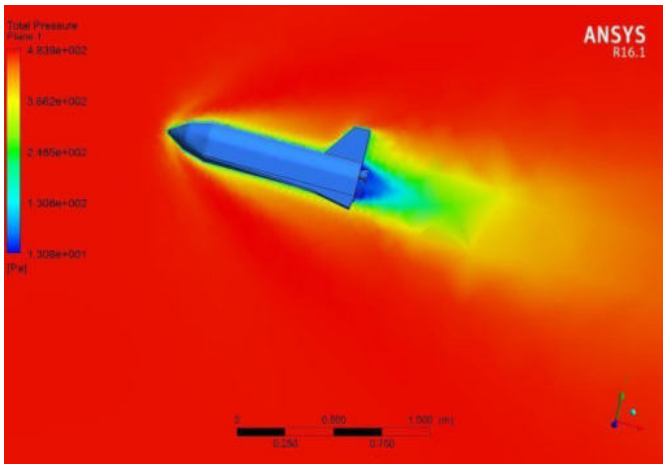

Fig.13 - Total Pressure Contour for ZrB_2 at Mach 1.5

4.9. Total Temperature Contour for ZrB_2 at Mach 1.5

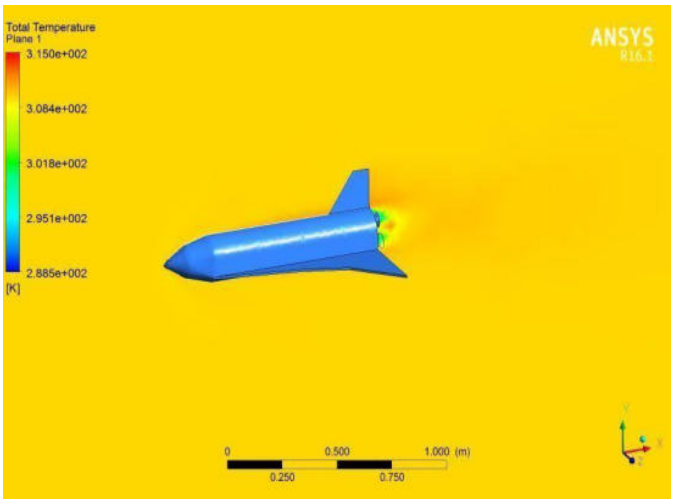

Fig.14 - Total Temperature Contour for ZrB_2 at Mach 1.5

4.10. Mach Number Contour for ZrB_2 at Mach 3

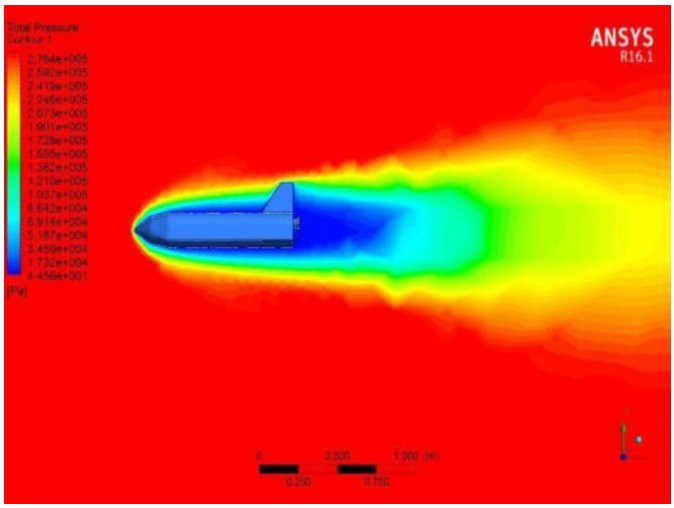

Fig.15 - Mach Number Contour for ZrB_2 at Mach 3

4.11. Total Pressure Contour for ZrB_2 at Mach 3

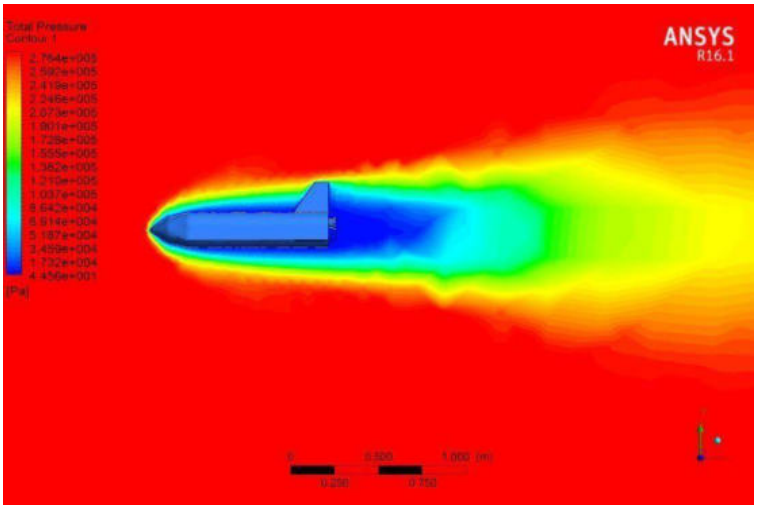

Fig.16 - Total Pressure Contour for ZrB_2 at Mach 3

Table 2 - $SiBr_2$ Temperature Fluctuations In °C

Mach No.	Nose	Wing bottom	Fuselage
1.5	227	283	309
3	387	402	421

Table 3 - ZrB_2 Temperature Fluctuations In °C

Mach No.	Nose	Wing bottom	Fuselage
1.5	243	299.2	322
3	392.5	423.5	448.7

5. Comparative Results

5.1. Nose

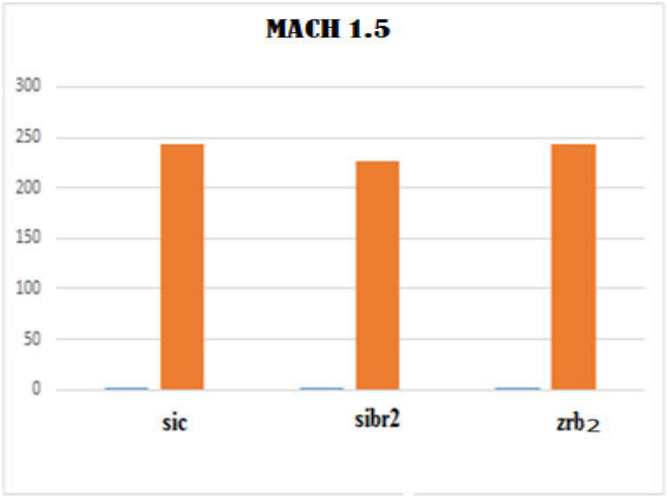

Fig. 17 - Mach No 1.5 Temperature Comparison At Nose

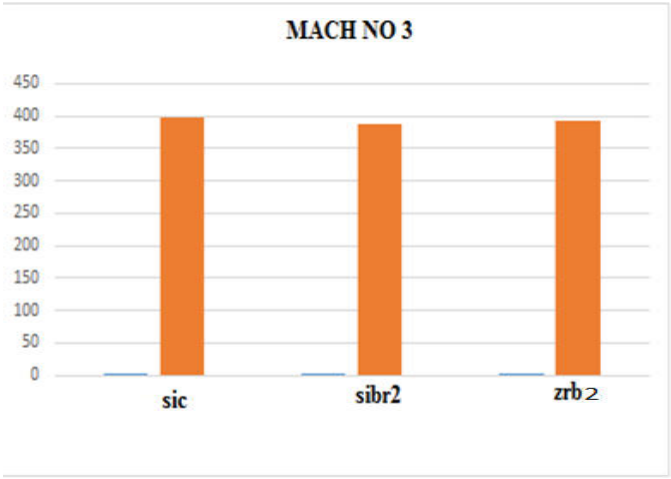

Fig. 18 - Mach No 3 Temperature Comparison At Nose

5.2.Wing

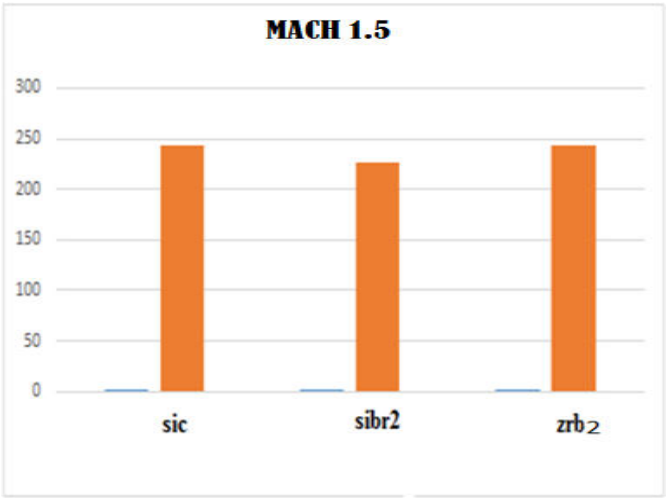

Fig. 19 - Mach No 1.5 Temperature Comparison At Wing

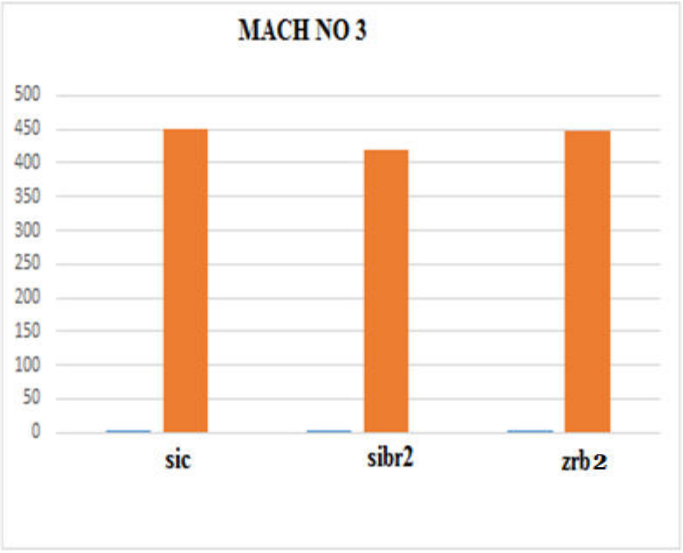

Fig. 20 - Mach No 3 Temperature Comparison At Wing

5.3. Fuselage

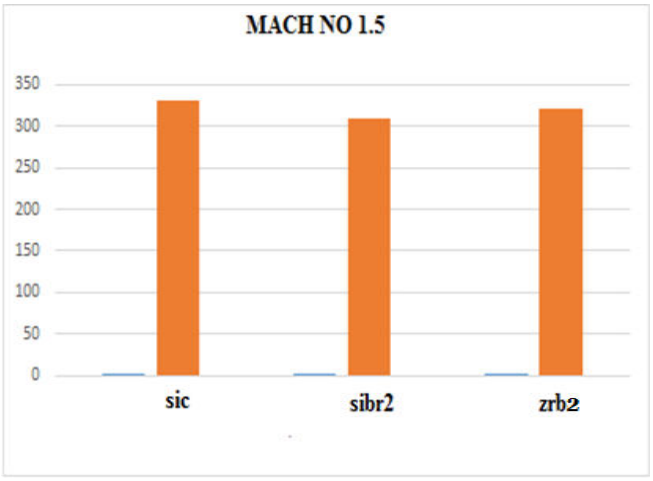

Fig. 21 - Mach No 1.5 Temperature Comparison At Fuselage

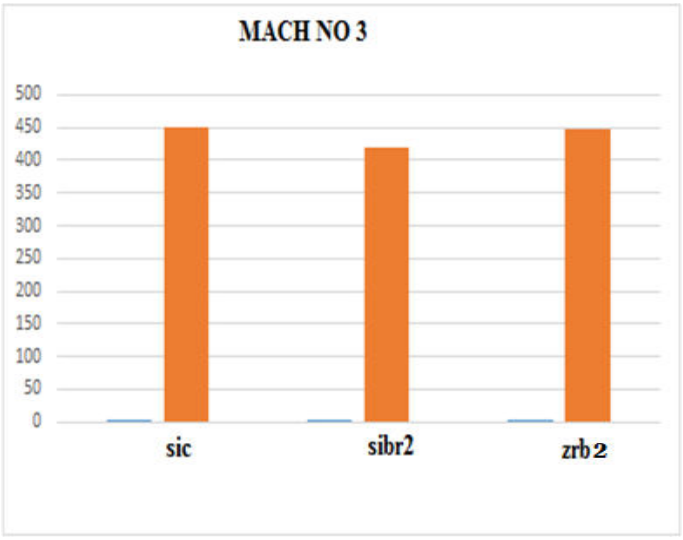

Fig. 22 - Mach No 3 Temperature Comparison At Fuselage

Table 4 – Mach 1.5 Temperature Comparison ℃

	Sic	$Sibr_2$	Zrb_2
Nose	247	227	243
Wing	292	283	299.2
Fuselage	332	309	322

Table 5 - Mach 3 Temperature Comparison ℃

	Sic	$Sibr_2$	Zrb_2
Nose	399	387	392.5
Wing	419	402	423.5
Fuselage	452	421	448.7

5. Conclusion

In this paper, two different materials (silicon dibromide & zirconium diboride) are analyzed at two different Mach numbers which are at supersonic

velocities. After comparing with the results, silicon dibromide is best suitable for nose, wing bottom and fuselage sections, as it has lower temperature effects than zirconium diboride. At high Mach number of vehicle, velocity of flow increased and the pressure of the vehicle decreases drastically. The temperature increases with increase in Mach number. Experimental and computational studies have been made to obtain the flow field over a typical RLV configuration. Computations made using CFX shows reasonably good comparison with experimental results and capture most of the features of flow field.

REFERENCES

[1] Aso, S., Tani, Y., Tadakuma, K., 2004. A Study on Aerodynamic Characteristics of LiftingBody and Wing Body Configurations for Fully Reusable Launch Vehicles, 34th AIAA FluidDynamics Conference and Exhibit, AIAA 2004-2536.

[2] Baiocco P., Guedron S., Plotard P., Moulin J., "The Pre-X Atmospheric Re-entry Experimental Lifting Body: Program Status and System Synthesis", 57th IAC Congress, Valencia, Spain, 2-6 October 2006.

[3] Computational Fluid Dynamics (CFD) In Launch Vehicle Applications" Practice No. Pd- Ap-1311"

[4] Epuri, S.K., 2009. Investigation of Flow field over a reusable launch vehicle and double delta wing at subsonic speed, M.E. Thesis, Birla Institute of Technology, Mesra, Ranchi.

[5] Kenji, T., Takuro, I., Aso, S., Tani Y., 2006. Experimental Studies on Lateral Blowing for the Improvement of Aerodynamic Characteristics of Reusable Launch Vehicle in Subsonic Flow, Memoirs of the Faculty of Engineering, Kyushu University, Vol.66(2) 179-196.

[6] Mendenhall, M. R., Chou, H. S. Y., and Love, J. F. Computational aerodynamic design andanalysis of launch vehicles. AIAA 2000-0385, Jan. 2000.

[7] Richmond, P.B., Delma, C.F., 1975. Subsonic and Transonic Dynamic Stability Characteristics of a Space Shuttle Orbiter, NASA Technical Memorandum, D-8042.

[8] Study of Coatings used in Gas Turbine Engine, INTERNATIONAL JOURNAL OF ENGINEERING RESEARCH & TECHNOLOGY (IJERT) CONFCALL – 2019 (Volume 7 – Issue 11).

[9] "Design and Analysis of Wedge Nozzle to Absorb the Sound Emission from the Jet Exhaust." International Journal for Scientific Research and Development 6.2 (2018): 1807-1810.

[10] "Design and Analysis of Quadcopter Frame and Propeller." International Journal for Scientific Research and Development 6.5 (2018): 250-252.